In Vivo Applications of a Molecular Computing-Based High-Throughput NIR Spectrometer

Lisa A. Cassis[a], Bin Dai[b], Aaron Urbas[b], and Robert A. Lodder[b*]
Graduate Center for Nutritional Sciences[a] and Department of Chemistry[a,b]
University of Kentucky, Lexington, KY 40506-0055

Abstract

Modern hyperspectral imaging is able to collect exceptional amounts of information at astonishing speed. Reducing these data from physical fields to high-level, useful information is difficult. Integrated computational imaging (ICI) is a process in which image information is encoded as it is sensed to produce information better suited for high-speed digital processors. Both spatial and spectral features of samples can be encoded in ICI. When spectral images are simultaneously obtained and encoded at many different wavelengths, the process is called hyperspectral integrated computational imaging (HICI). Lenslet arrays and masks are ideal for encoding spatial features of an image. This process is used here to analyze motion and metabolism in freely moving rats. Complex molecular absorption filters can be used as mathematical factors in spectral encoding to create a factor-analytic optical calibration in a high-throughput spectrometer. This process is used here for remote sensing of ethanol concentrations. In this system, the molecules in the filter effectively compute the calibration function by weighting the signals received at each wavelength over a broad wavelength range. One or two molecular filters are sufficient to produce a detector voltage that is proportional to an analyte concentration in the image field. Because a single detector voltage can reveal analyte concentration, HICI is able to calculate chemical images orders of magnitude more rapidly than conventional chemometric approaches.

Keywords: Integrated computational imaging, hyperspectral imaging, lenslet arrays, spatial feature encoding

Introduction

Modern hyperspectral imaging is able to collect unprecedented amounts of information with extraordinary speed. Remote sensing with combinations of SAR, IR, UV/visible and similar technologies is increasingly prevalent, adding to the computational burden. Reducing these volumes of data from physical fields to high-level, useful information is difficult. Part of this reduction is now being done optically. In the past, optics has served mainly to render the universe more easily visible to human observers. Now, computers are increasingly employed to make sense of the visual world in ways that humans cannot. With a new generation of optics, scientists and engineers are recasting visual scenes for interpretation exclusively by computers. To the human eye, these pictures appear distorted at best, or at worst look like visual noise, without discernable meaning. Nevertheless, to computers, such data are worth more than a thousand words. Optimizing complete vision-and-action systems for computers lies at the core of *integrated computational imaging* (ICI)[1]. Computers are well-established manipulators of digitized images, and image-processing programs do it routinely on desktop machines. However, what is new is the strategy of ICI - *processing image information as it is sensed* to make it better suited for the "computer mind."

Both *spatial* and *spectral* features of samples can be encoded in ICI. When spectral images are simultaneously obtained and encoded at many different wavelengths, the process is termed hyperspectral integrated computational imaging (HICI). Molecular absorption filters can be used as mathematical factors in spectral encoding to create a factor-analytic optical calibration in a high-throughput spectrometer. In this system, the molecules in the filter effectively compute the calibration function by weighting the signals received at each wavelength over a broad wavelength range. Lenslet arrays and masks can also be employed to encode spatial features of a hyperspectral image. This paper describes spectrometer designs that use molecular-computing to replace traditional principal component analysis in a computer with molecular filters tailored to produce factor scores at the detector, and spectrometer designs that use lenslet arrays to extract and encode selected image features.

A simple analogy suggests the advantage of doing as much of the processing as possible in the sensing transducer itself. Imagine two gunfighters on Main Street at sundown in the old “wild west.” The first gunfighter’s hand and revolver are controlled by his brain using image information transmitted from the retinas of his eyes. Impulses must travel from his eye to his brain, and then from his brain to his hand. The second gunfighter’s hand and revolver are

controlled directly by the retinas of his eyes using nerve impulses that travel only one path instead of two. The second gunfighter's weapon is likely to always be slightly ahead of the first's. Moreover, the second gunfighter's brain is free to consider other, more effective strategies.

Spectral Feature Encoding with Molecular Computing: *Principal Component Analysis (PCA) methods.*

Many different variations contribute to the spectrum of actual samples, typically more variations than contribute to spectra of synthetic standards prepared in the laboratory. Field samples contain variations from instrument differences such as detector noise, differences in the constituents in the sample mixtures, interactions between constituents, shifting environmental conditions that influence the spectral baseline and overall absorbance, and differences in sample preparation and presentation[2]. In spite of these compound changes taking place, there should be a limited number of independent variations taking place in the spectral data. With a bit of luck, the largest variations in the calibration set will be the changes in the spectra due to the property you wish to measure, e.g., the different concentrations of the constituents of the mixtures. The strategy in traditional principal component analysis and in molecular computing of factors is to focus on the spectral variations in the calibration set. It is possible to compute a set of "variation spectra" that correspond to the differences in the absorbances at all the wavelengths in the spectra. In molecular computing, the molecular filters are selected to maximize the integrated differences in the variation-spectra within a certain bandpass. In PCA, the so-called variation-spectra can be used in place of the raw spectral data for constructing the calibration model. Usually there are fewer common variations in these PC or MFC spectra than the total number of calibration spectra, and so the number of computations required for the calibration equations is reduced, too.

If properly constructed, the "variation spectra" can be used to reconstruct the original spectrum of a certain sample by multiplying each variation-spectrum by a unique constant scaling factor and summing the results until the new spectrum agrees with the unknown spectrum. In principal, reconstruction can be done in either traditional PCA or molecular factor computing (MFC). Each spectrum in the calibration set must have a distinct series of scaling constants for each variation because the concentrations of the constituents are dissimilar. For this reason, the fraction of each "spectrum" that must be added to reconstruct the unknown spectral data is associated with the concentration of the constituents.

In PCA, the spectra of the variations are termed eigenvectors, or loadings, spectral loadings, loading vectors, or principal components or factors, based on the means used to compute the spectra. Regardless of the means, a simple transformation will convert one into another (eigenvectors into loadings, for example). The scaling constants employed to reconstruct the individual spectra are commonly called scores. Ordinary spectroscopy and PCA chemometrics records signals with a narrow bandpass at each wavelength and then weights the signals a at each wavelength λ with a coefficient f in a computer.

$$\text{score} = f_1 a_{\lambda 1} + f_2 a_{\lambda 2} + f_3 a_{\lambda 3} + \ldots \qquad \text{eq 1}$$

However, it is also possible to weight each wavelength in a spectrum optically using the absorbance spectra of "filter" molecules. The "scores" can then simply be read by an A/D as the voltage from a detector unit by integrating the total light through the sample and filter over a broad wavelength band. In this case, while the scores are not perfectly orthogonal, they are often close enough to permit chemical analyses to be performed. For those who question the lack of orthogonality, it is worth remembering that the principal component scores calculated on spectra in a traditional computer are also not perfectly orthogonal as soon as one new sample is added to the calibration set. Yet even in these cases, chemical analyses can usually be successfully performed.

Because the computed eigenvectors were generated from the original calibration spectra, the eigenvectors must relate by some means to the concentrations of the constituents that comprise the samples. The identical loading vectors can be used to predict "unknown" samples; therefore the only difference between the spectra of samples with different constituent concentrations is the fraction of each loading vector added (the scores). Using MFC, the only difference between the spectra of samples with different constituent concentrations is the integrated detector response in the wavelength bandpass, which is equivalent to a factor score as described earlier. Varying the bandpass for different types of samples can help to spread the scores, effectively improving S/N.

By PCA or MFC, the scores are exclusive to each independent principal component (or factor) and training-set spectrum, and can be used in lieu of absorbance values in either of the typical modeling procedures (classical least-squares, CLS, or inverse least-squares, ILS). Because the description of mixture spectra is condensed from many wavelengths to a small number of scores (illustrated in Fig. 1), spectroscopists usually apply the ILS manifestation of Beer's Law in computing concentrations because of its ability to calculate concentrations in the midst of interfering species. Of course, ILS preserves the averaging effect of CLS chemometrically by building a large number of

wavelengths from the spectrum (indeed, up to the entire spectrum) into the model when calculating the eigenvectors. As a result, factor models really combine the best features of both the CLS and ILS methods simultaneously in the one series of computations. This synergy is the primary cause for the generally better statistical performance of factor models over classical models in terms of robustness and accuracy

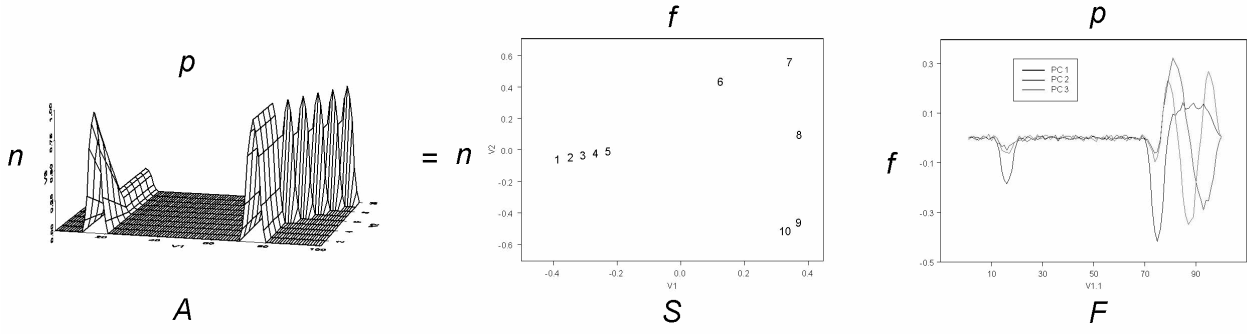

Fig. 1. PCA decomposes the spectral data into the most common spectral variations (often called factors, eigenvectors, or loadings, and basically equivalent to multiplex bandpass molecular filters) and the corresponding scaling coefficients (scores, equivalent to the integrated bandpass detector signal in MFC). A=original spectra, S=PC scores, F=factors (loadings), n=number of spectra, p=number of data points, f=number of PCs

The "secret" in these modeling methods is in the technique by which the eigenvectors are obtained. These models build the concentration predictions upon changes in the data, not absolute absorbance values (absolute absorbance values are used in the classical models). To calculate a PCA model, the spectral data must vary in some fashion. The simplest way to achieve variations in the spectra is to alter the concentrations of the constituents. When making these alterations, problems can arise with collinearity, just as can occur with ILS modeling. Collinearity is easy to understand: If the concentrations of two constituents in the calibration samples are always present in the same ratio in the samples (for example, 3:1 of chemical X to chemical Y), then the modeling process will only detect one variation instead of two. Constant ratios sometimes arise in building calibration sets when a series of dilutions are made from a single stock solution. The model "sees" all the absorbance peaks of constituent X increase or decrease together with constituent Y. As a result, only one variation is sensed: the changes in the spectrum of the sum of X and Y. For this reason, when calibrating models it is imperative that the concentrations of the individual constituents of interest be present in uncorrelated and evenly distributed ratios. The same basic principle holds whether calibration is done optically by MFC, or digitally in a computer (like PCA).

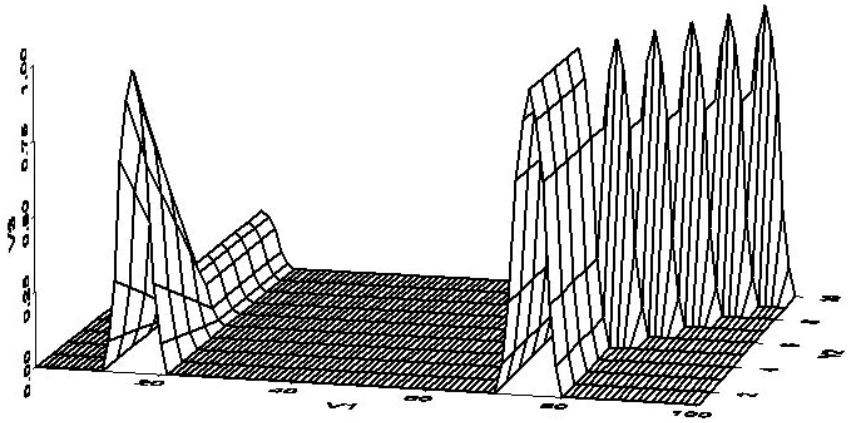

Fig. 2. A hypothetical training set of spectra with two varying constituents. The peak on the left changes height while the peak on the right is held constant. Then the peak on the right drifts to higher energies while the intensity of the peak on the left is held constant.

Spectral data are often mean-centered prior to PCA being applied to a calibration set. Mean centering is performed by calculating the mean spectrum (i.e., average spectrum) from all of the calibration spectra, and then subtracting the mean spectrum from every calibration spectrum. Mean centering enhances slight differences between the spectra being centered, rendering the differences more easily visible. Bear in mind that computerized factor analytic methods compute the principal components based on variations in the absorbance data, and not the absolute absorbance values themselves. For that reason, any transformation that increases the likelihood of detecting differences between the calibration spectra will enhance the model. Mean-centering can be understood from the perspective of PCA calculating the eigenvectors. Because the eigenvectors correspond to the variations in the spectral data that are shared by all the calibration spectra, eliminating the mean merely removes the first, most common variation before the data are handled by the PCA code. Similarly, double-beam spectrometry can be thought of as a way of mean-centering spectral data optically, too. In MFC, a similar enhancement can be obtained by moving the limits of detector integration (the bandpass) to regions of the spectra where those same slight differences used in PCA occur. In fact, in PCA limiting a calibration to such spectral regions often improves standard errors of estimate (SEE) and standard errors of performance (SEP).

PCA is actually a process of elimination, iteratively removing each orthogonal variation from the calibration spectra sequentially to generate a group of eigenvectors (principal components) that correspond to the variations in the absorbance values that are shared among all spectra. In reality, the underlying variations are seldom actually independent, and removing them orthogonally to form the inside model space leaves a "reverse impression" of them on the outside model space. MFC filters are also never completely orthogonal for physical reasons. Sometimes this means that fewer MFC factor filters are needed than PCs in PCA, but sometimes not. Once the calibration data have been treated completely by the PCA algorithm, the data are reduced to two matrices: the eigenvectors (dimensioned like the spectra) and the scores, which act as scalar eigenvector weighting values for all the calibration spectra. The matrix expression of the model equation for the spectral data appears in the form:

$$A = S\ F + E_A \qquad \text{eq 2}$$

where $\boldsymbol{A}$ is an $\boldsymbol{n}$ by $\boldsymbol{p}$ matrix of spectral absorbance values (as in Fig. 2), $\boldsymbol{S}$ is an $\boldsymbol{n}$ by $\boldsymbol{f}$ matrix of score values for all of the spectra, and $\boldsymbol{F}$ is an $\boldsymbol{f}$ by $\boldsymbol{p}$ matrix of eigenvectors. The $\boldsymbol{E_A}$ matrix is the errors in the model's ability to predict the calibration absorbance values and has the same dimensionality as the $\boldsymbol{A}$ matrix. In the case of eigenvector analysis, the $\boldsymbol{E_A}$ matrix is often called the matrix of residual spectra. The dimensions of the matrices are representative of the data they hold; $\boldsymbol{n}$ is the number of samples (spectra), $\boldsymbol{p}$ is the number of data points (wavelengths) used for calibration, and $\boldsymbol{f}$ is the number PCA eigenvectors. Similarly, in MFC $\boldsymbol{S}$ is obtained by integrating the total light through the sample and individual MFC filters over a broad wavelength band. $\boldsymbol{F}$ are the filter spectra, and $\boldsymbol{E_A}$ are the errors in the model's ability to predict the calibration absorbance values. Fig. 3 shows how spectra in Fig. 2 can be reconstructed from factor scores so they can be compared to spectroscopic predictions made by modeling programs like Gaussian.

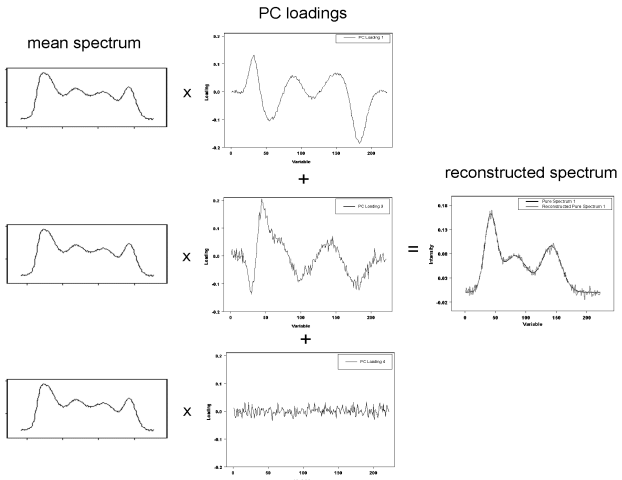

Fig. 3. The original calibration spectra can be recreated using all of the loadings and scores. By selecting certain vectors from the

loadings, the spectra of selected constituents or properties can be selectively reconstructed. Molecular filters MF1 and MF3 could be substituted for PC1 and PC3, and the scores would be the integrated detector signals observed with MF1 and MF3.

MFC-computing molecules are selected by comparing the spectrum of prospective filter materials to the loadings spectra calculated by PCA. Given a set of training spectra collected at all available wavelengths, it is possible to rationally select molecular filter (MF) materials to perform PCA. PCA is designed to maximize the signals from the spectral regions with the most variability by most heavily weighting them in calibration. However, PC loadings heavily weight signals in the positive and negative direction, which cannot be done with MFs without offsetting signal gained at one wavelength with signal lost at another wavelength in the total bandpass. Because only absolute values can be represented in MFs, as many as two filters are needed for a PC, one for the positive loadings (MF1) and one for the negative loadings (MF2). The transmission spectrum (%T) of the filter material should be as similar as possible to the absolute value of the loadings spectrum being targeted. Using a conventional spectrometer, mixtures of liquid molecular filters can be titrated to produce the optimum PC result.

PCA and MFC share a number of important advantages over more established spectroscopic techniques. Neither PCA nor MFC require wavelength selection. Any number of wavelengths can be employed in calibration; typically, the entire spectrum is used with PCA, and large ranges with MFC. Using more wavelengths provides an averaging effect that produces a model less susceptible to spectral noise. Both PCA and MFC provide spectral data compression and permit use of inverse regression to calculate model coefficients. Each technique can be calibrated to measure constituents of interest while ignoring most interference, and can be applied to complex mixtures because only calibration information on the constituents of interest is necessary. In some cases, they can even be used to identify samples containing contaminants not present in the original calibration mixtures.

PCA and MFC each present special problems that must be considered in their use. PCA computations are slower than the molecular computing approach to estimating scores, which is effectively instantaneous. The calibration models produced by these two techniques are relatively complex, and can be difficult to interpret and understand. Optimization of models requires some knowledge of PCA and knowledge of MFC that is not yet complete. Nonlinear spectral effects in complex samples sometimes be linearized with careful choice of molecular filters in MFC, and with PCA can be modeled in software like Gaussian to trace their source. PCA vectors often do not correspond directly to constituents of interest. In MFC, filter molecules can be selected that correspond directly to sample constituents, but only for the sample constituents that are known. From time to time spectroscopy senses an effect that is merely correlated to a constituent of interest instead of originating from the constituent itself (this usually shows up as absorbance signals at unexpected wavelengths.) For this reason, analytical chemists seldom rely on a single instrumental technique to analyze a sample. Other analytical methods can be used on these samples to verify results where accidental correlation is suspected. Generally, a large number of samples are required for accurate calibration. In hyperspectral imaging, however, each pixel contains an entire spectrum so large numbers of spectra are easy to obtain. Gathering sufficient calibration samples can be problematical when one must avoid collinear constituent concentrations. However, computer methods for assisting in the collection of orthogonal samples exist to ameliorate this problem.

Spatial Feature Encoding with Lenslet Arrays and Masks

Abandoning the customary concave and convex disks, optical engineers in ICI are building strangely shaped, fundamentally different lenses adapted to the strengths of computers. Arrays of light pipes can process optical data in ways that lenses cannot. These optical components diverge from the traditional approach in which lenses form something humans recognize as an image. In nature, there are beetles that navigate by sensing certain wavelengths or polarizations of light in air without forming an image from the data. Scientists have been slow to explore such alternative sensors, however, because they have traditionally modeled optical instruments such as cameras after our own image-rendering eyes.

The revolution in integrated computational imaging extends beyond just lenses and light pipes. A new trend in hyperspectral imaging is to speed the visual data processing and reduce data storage requirements by downloading some of the computation to the sensing detector itself. In many cases, the detector array can perform both feature extraction (of both physical and spectral features) and encoding of these features. The codes are transmitted by the array to the computer, integrating the computation and imaging to reduce the huge data load and speed the processing. Similarly, molecular computing in a multiplex image bandpass spectrometer can accomplish hyperspectral imaging as integrated computational imaging performs feature extraction.

Current sensor system architectures detect signals from a physical stimulus, convert them to electrical signals, convert the electrical signals to digital form for processing by computers, and, finally, extract critical information from the

processed signals for exploitation. Integrated Sensing and Processing (ISP), an initiative launched in the Defense Advanced Research Projects Agency[3], aims to replace this chain of processes, each optimized separately, with new methods for designing sensor systems that treat the entire system as a single end-to-end process that can be optimized globally. In the 21st century, global information dominance is necessary to protect U.S. air, space and ground assets. Sensor systems like interferometric synthetic aperture radar (InSAR) and IR video collect unprecedented amounts of data, greater than 10^{12} pixels/day that require more than 10^{16} flops/day to process. At the same time, the "downsizing" personnel trend persists and the ratio of "pixels to pupils" is heading toward infinity. These trends combine to make training data collection, processing, downlink and distribution all problematic as the U.S. military seeks ways to reduce rapidly data from physical fields to high-level information. At the same time, computing resources are limited in size, weight, power, and cost. Application Specific Integrated Circuits (ASICs) do not really help because they solve a fixed problem in a changing sensor/target environment. ASIC design time and cost tend to be prohibitive. More flexible detection schemes like the Texas Instruments digital micromirror array (DMA) measure features, not pixels, under computer control[4]. This holistic approach boosts signal-to-noise ratio (SNR) and concentrates information the way ICI was intended to do.

The Texas Instruments DMA chip was originally designed for use in consumer televisions, home theater systems and business projectors. White light passes through a color filter wheel, causing red, green and blue light to be directed in sequence on the surface of the DMA. The micromirrors have only two positions, on and off. The switching of the mirrors, and the proportion of time they are 'on' or 'off', is synchronized according to the color illuminating them. The human visual system integrates the sequential colors and registers a full-color image in the brain.

ICI with a DMA requires only simple computing because the feature extraction and encoding is done by the detector array. In contrast to calculating Longbow classifiers, Fourier-Mellin transforms, SVDs, and PCAs with powerful digital computers, in ICI simple digital manipulations and analog detection permit low-cost, rapid identification of targets. To provide an example, let us assume that a target is shaped like a rectangle (see Fig. 4).

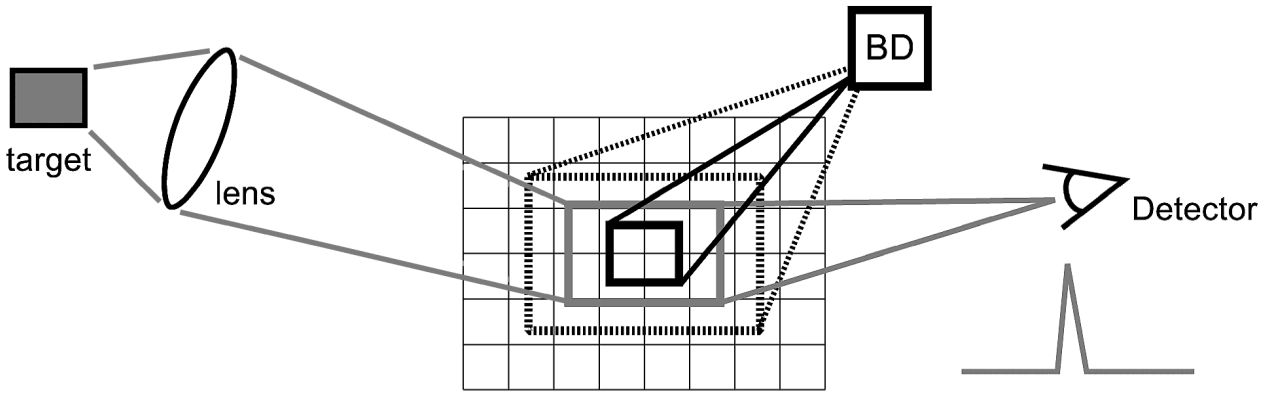

Fig. 4. A digital micromirror array can be programmed to measure the relevant features of a target directly.

A lens projects an image of the target on a DMA. When DMA elements are 'on', they reflect light into a detector. When the elements are 'off', they reflect light into a beam dump. A small rectangle is turned on first (see a), then its elements are turned off and the next largest size target shape elements are turned on (see b). This process is continued progressively until the target shape completely fills the DMA (see c and d). When the DMA target shape and size exactly match the target image projected on the array by the lens, a signal spike appears at the detector. At this point, the ICI system has identified the target through selective feature extraction. In addition, the range to the target has been calculated because the scale of the actual target is known, and the range is identified by size of the projection creating the signal spike at the detector.

The same DMA technology can be employed to compute principal components optically. For example, using a lens to collimate light for a transmission grating, a spectrum can be projected across a DMA. In this example, the columns of the DMA represent wavelength, and the rows reflect a fraction of light (between zero and one) collected at each wavelength. Principal components are simply a weighted sum of light intensities across a range of wavelengths, and it is a simple matter to turn on a fraction of the mirrors in each column to represent the weighting at each wavelength. By employing this scheme, the signal observed at a single analog detector can be easily related to a principal component

score, and even to an analyte concentration. Thus, a relatively complex computational function is reduced to measuring the voltage on a single detector.

Algorithms for design and operation of ICI sensor systems are being developed that allow back-end exploitation operations, such as target identification and tracking, to configure and set the operating modes of sensor elements without human intervention to ensure the most significant data are always being collected as scenarios evolve. The ISP program approach is leading to an order-of-magnitude performance improvement in detection sensitivity and target classification accuracy, with no change in computational cost, across a broad range of Department of Defense (DoD) sensor systems and networks - from surveillance to radar, sonar, optical, and other weapon guidance systems. ISP has created novel feedback strategies to administer the elements of an adaptive optical sensing system. ISP has invented new mathematical frameworks for global optimization of design and function of a number of diverse types of sensor systems. It is also realizing its software prototypes of ICI methodology in test-bed hardware systems, including missile guidance and automatic ground-target recognition modules.

Stepping away from military applications, researchers are also replacing conventional optics on microscopes and other optical instruments, and at the same time imparting extended depth of field to these devices. Other optical engineering groups are developing ICI optics to facilitate computers in sensing motion and the physical properties of remote objects. Exceeding the limits of visible light, engineers foresee construction of similar lenses that can process other segments of the electromagnetic spectrum, extending the general change in the way scientists think about sensing.

Extending depth of field computationally has applications in standard cameras, microscopes, and other optical instruments that use collections of convex and concave lenses to focus light onto flat electronic detectors or sections of film. An autofocus camera normally moves the positions of certain of those optical elements forward and backward until a sensor that observes contrast differences in the field of view distinguishes satisfactory detail. Doing away with autofocusing and reducing component count of optical sensing systems begins by considering any panorama observed through a lens as a computer would: as a mosaic of miniature illuminated points. Paradoxically, removing autofocusing systems relies on a defocusing lens. Instead of counting on a mechanically movable lens to focus light, a saddle-shaped lens is kept motionless. This warped lens submits what looks to be a blurred image to a computer, which then runs an algorithm that reconstructs the image point by point. Together, these two parts are labeled wavefront coding by the inventors at CDM Optics[5]. The ICI product of this warped lens (see Fig. 5) and computational reconstruction is an image in sharp focus in the foreground and background simultaneously.

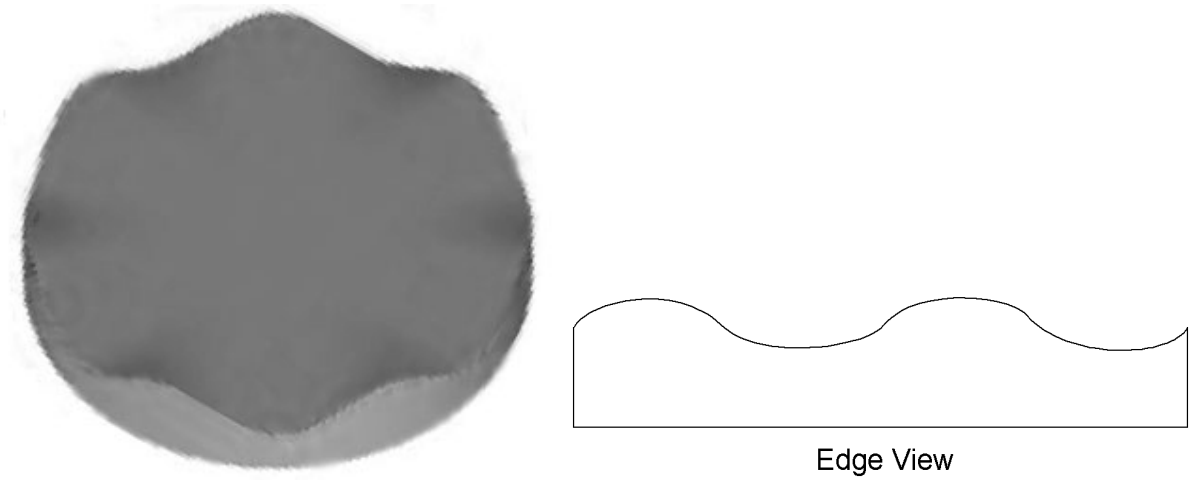

Fig. 5. A wavefront coding lens. The undulating surface is calculated to blur images consistently before computerized blur removal. The undulations are magnified by 10^4 to render them visible in the figure.

The extended depth of field produced by wavefront coding (at least 10 times greater than the depth of field for conventional lenses), does involve compromises. As the computer eliminates the general blurring initiated by the ray-altering lens, it introduces a modicum of random noise, which may appear as faint coarsening of smooth surfaces. On the other hand, the enhancement of overall focus overshadows the slight effect of that noise on the image. Furthermore, added computer processing can remove that noise.

Innovative commercial products that feature ICI in the form of wavefront coding technology include modules for microscopes and extended depth-of-field endoscopes for minimally invasive surgery as well as manufacturing. Because ICI can also correct common lens aberrations as wavefront coding is used to de-blur the image, the ICI methodology presents a means to cut the number of aberration-correcting optical elements installed in typical cameras and further devices. For example, lightweight space telescopes can be manufactured with loose construction tolerances using wavefront coding technology.

Wavefront-coding lenses represent only a few of the innumerable possible forms of ICI. For example, insect eyes suggest sensing using arrays of miniature conventional lenses, also known as lenslets. In this form of sensor, every lenslet focuses a small, low-resolution image onto a segment of an electronic detector at the rear of the lenslet array. Using all of the lenslets' various perspectives, ICI can compute a single large scene at approximately twice the resolution than would be possible if a single traditional lens had been employed. A unique advantage of the ICI lenslet approach is that the already thin lenslet array can focus light onto a detector only micrometers away. This extreme reduction in focal length has been used to develop a prototype ICI camera as thin as a microscope slide[1].

Other lenslet arrays are even simpler, using only apertures instead of lenses. For example, a miniature opaque polymer block packed with specifically angled holes that act as light pipes allow photodetectors behind the block to collect light from a scene concurrently from different viewpoints. The product is an ICI device that can reconstruct the motion of an enemy asset like a truck or personnel carrier without obtaining or examining any real images of the vehicle. Nearly all existing motion-tracking devices obtain complete images of a two-dimensional scene and then use the computer to scrutinize pixel configurations in search of variations signifying motion. The search is a time-consuming, computer-intensive process and prone to a variety of errors. With this new multi-aperture ICI device, light from a target object arrives at the detectors in the form of a characteristic optical code from which a computer can rapidly reconstruct motion with negligible computations. This approach is described later in more detail in connection with metabolic monitoring of freely moving rats.

Hyperspectral ICI optical elements have been designed for collecting all of the spectra at the same time across the pixels of a complete scene. Hyperspectral data may expose camouflaged armaments in a satellite image or biological activities under a microscope, especially with the assistance of fluorescent labels that bind to particular cellular structures. For example, one ICI spectra-capturing lens generates a multicolor (multiwavelength) design in which a 30-color spectrum linked with each point in a scene is mapped onto a detector. The design is not an image at that point; it is only a disorderly collection of colors and pixels. In spite of this disorder, computerized sorting can transform the apparent visual disharmony into an image of the scene at any individual wavelength. Such hyperspectral data have become one of the most important means by which scientists analyze the physical and chemical properties of objects extending from atoms to distant planets.

More than a generation ago, scientists tried to use lenses to transcend simple imaging. DoD tried to exploit "optical correlators" that could sense threats by optically comparing reconnaissance pictures with patterns of enemy vehicles stockpiled holographically. At the time digital processing was new but unsophisticated, and the most elegant method to manage the data was to process it optically. Regrettably, the tactic was unsuccessful because optics did not afford the degree of accuracy required for detecting threats in complex and chaotic battlefield scenes. Technology has improved significantly since that time. Most noticeably, the data-analysis capabilities of computers have skyrocketed. However, there have also been important developments in mathematical tools and innovations in optics manufacture that permit more complex lenses to be prepared, such as the wavefront coding lenses and aperture arrays using light pipes. With the union of the latest computers and innovative optics, ICI is ready to reveal a universe of possibilities that have long been concealed from the human eye.

Our laboratories contain an assortment of monochromator-based spectrometers, FT instruments, and tunable lasers that are used for routine spectrometric work. These instruments function adequately in ordinary applications. However, when high sample throughput is required, such as when pharmaceutical process analytical technologies (PAT) are used to examine finished dosage forms for zero-defect process control, traditional instruments can perform poorly. These older instruments require too much time to acquire data, and produce too much raw data that must be analyzed to provide high-level information. Hyphenation of analytical methods (e.g., NIR/ARS, or NIR/acoustic-resonance spectrometry) further increases the data burden, and the time needed to acquire spectra[6]. Furthermore, traditional instrumentation can be too complex and heavy for some applications, such as remote sensing using robotic platforms on distant planets. ICI goes a long way toward solving these problems with traditional instruments. Use of MFC in the optical design of instruments reduces the total amount of data that must be analyzed as it reduces the total instrument part count (there is an approach in ARS that is similar to MFC, but is beyond the scope of this article). Simpler instruments

are often more rugged than complex instruments, and lighter and more suitable for applications like astrobiological research.

Spectral Feature Encoding of Ethanol and Aneurysm with Molecular Computing

Fig. 6 is a diagram of a prototype MFC spectrometer that has been constructed based on an earlier design[7]. A 12VDC, 25-watt tungsten-halogen lamp provided broadband near-IR illumination. The source was powered by a stabilized DC power supply. An optical chopper modulated the near-IR beam at 210 Hz. A lock-in amplifier provided phase-sensitive detection. A lead-sulfide detector (CalSensors, Inc.) with an active area of 1x1 mm was placed near the focal point of the near-IR beam.

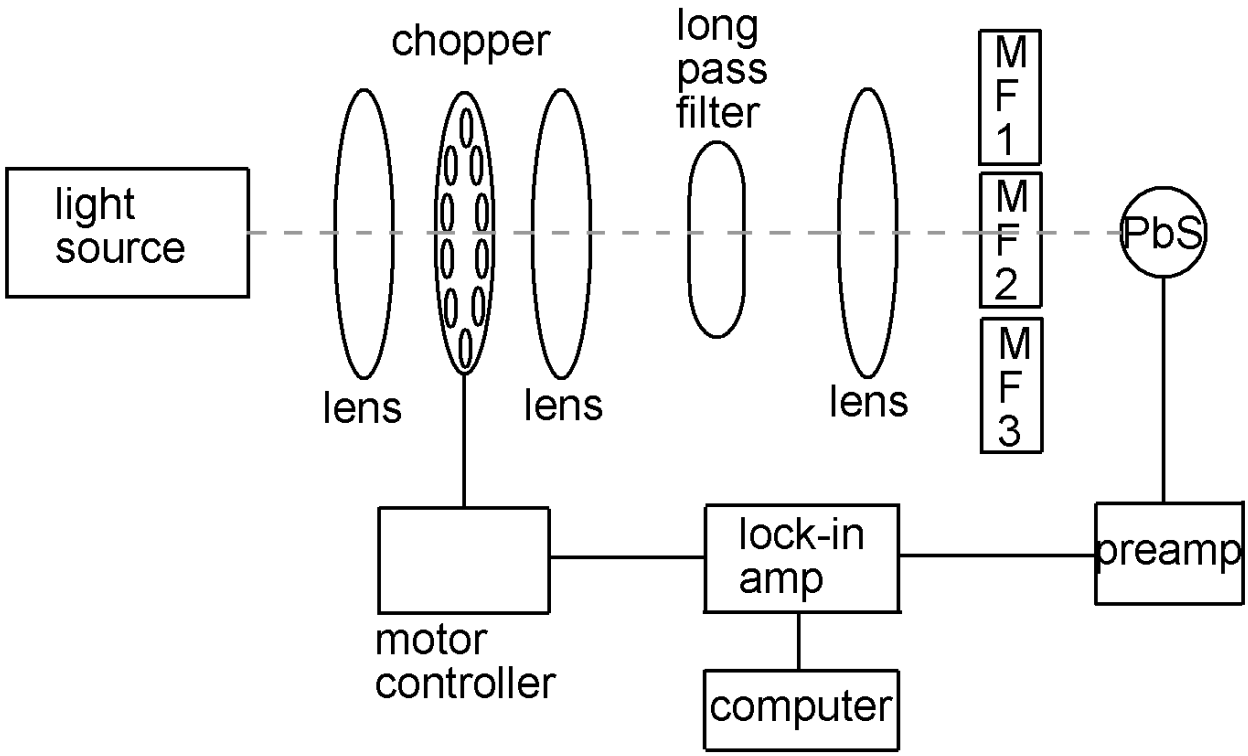

Fig. 6. Block diagram of a prototype molecular computing near-IR spectrometer that outputs factor scores. Three molecular filters (MF1, MF2, and MF3) rotate in and out of the light path on a filter wheel.

In general, near-IR absorption signals grow weaker as the wavelength of the radiation decreases. Each consecutive order of overtone or combination band is approximately a factor of ten weaker. A filter pathlength of one cm was selected for operation in the near-IR range from 1200-2400 nm. In this wavelength range, most organic liquids attenuate radiation almost completely at their absorption peaks at a 1-cm pathlength (i.e., in a molecular computing context, absorption peaks place zero weight on signal values in the factor score). The majority of these liquids also deliver sizeable bands of radiation within these limits of pathlength and wavelength (i.e., in a molecular computing context, these bands place nonzero weight on signal values in the factor score). At wavelengths lower than 1200 nm, most molecules fail to absorb strongly enough to attenuate significantly the near-IR beam in a reasonable pathlength. In addition, the tungsten-halogen light source has the most radiant power at shorter wavelengths. A 1200-nm long-pass filter was installed to prevent overwhelming the detector with light containing only modest sample information on these grounds.

Molecular filters can be held on a track or on a wheel. The sample cuvette was placed immediately in front of the filters and the PbS detector directly behind them. Black baffles (not shown in the figure for simplicity) were employed to avoid stray modulated light escaping around the sample and filters. The baffles were found to be very valuable, particularly whenever the samples or the filters were strong light absorbers. In either case, even a minute quantity of stray light can lead to appreciable errors. The convex lenses were situated to produce a defocused 1:1 image of the

source filament on the active area of the detector. The small defocusing was necessary because inserting the filters and samples in the beam path shifted the focal point of the filament image forward.

Absorbance values were computed using the conventional $\log(I_o/I)$, although Beer's Law should not be projected to apply when broadband radiation is used for measurements. I_o was calculated using a solvent matrix blank. The filter substances used for MFC include ethanol, polymethylmethacylate (Plexiglas), aniline, acetone, cyclohexane, polystyrene and water. However, any substance with an absorbance spectrum similar to the principal component loadings over the measured spectral region will suffice (see Fig. 7).

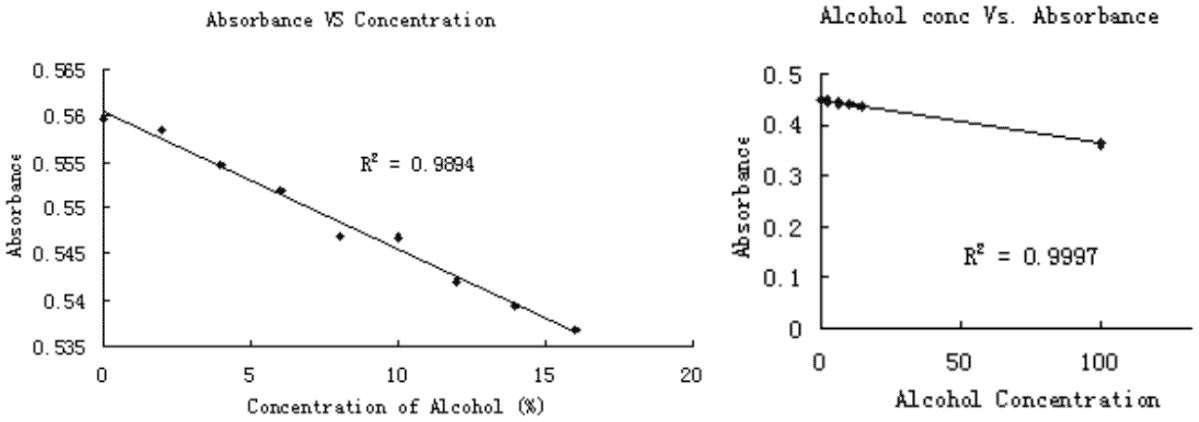

Fig. 7. Ethanol concentration in water measured using only one molecular filter factor.

Our group has already constructed a constant-height near-IR near-field scanning optical microscope (NSOM) using an external cavity tunable diode laser as a light source (80 nm tuning range per diode). This NSOM used a single-mode optical fiber pulled in a special oven to a tip diameter of 100 nm. This instrument has been utilized to demonstrate the feasibility of spectrally imaging single low-density lipoprotein (LDL) particles (18-25 nm in diameter). Furthermore, electromagnetic models have been developed and proven with experimental results to explain novel near-field imaging effects[8].

However, *NSOM scanning is a slow process* because only one point on the sample surface can be scanned at a time with the optical fiber tip. Moreover, a tunable diode laser must slowly scan a range of wavelengths at each point on the sample. Replacing the tunable diode laser in the NSOM with synchrotron light, and placing molecular filters in the synchrotron beam path before coupling the light to the single-mode optical fiber, may enable the NSOM scanning process to be speeded up substantially. This new instrument could be used to examine collagens and elastin and their distributions in mouse aortas. A number of genetic "knockout" murine models have been developed recently to mimic human atherosclerosis and abdominal aortic aneurysm (AAA)[9]. Techniques for monitoring the onset, progression, and regression of these processes in murine models could provide valuable pathophysiological insights into the disease processes. Nondestructive in vivo techniques will be needed for proteomics studies in these models. Finally, these analytical methods may be useful in assessing the effectiveness of possible treatments.

A synchrotron is a huge machine by most laboratory standards, and it produces very intense light comprising many different wavelengths[10]. The electromagnetic radiation is considerably more intense than that from a diode in a near-IR TV remote control, a microwave oven, or dental X-ray machine covering the same wavelengths, because the synchrotron's rays of light are concentrated into very small zones. These small areas are ideal for multiwavelength microscopy in the near and far fields. The synchrotron produces light by accelerating electrons to nearly the speed of light. Magnets channel the electrons into circular paths. As the electrons turn (accelerate), photons are emitted. The mechanism of the Brookhaven National Laboratory National Synchrotron Light Source includes an electron gun, linear accelerator, a circular booster ring (to increase the speed of the electrons), two storage rings (to re-circulate electrons), and beamlines (evacuated pipes down which the infrared, UV, and X-rays are launched to the research areas where they are used for experiments).

Nanometer-sized structures are becoming increasingly important and, as a result, near-field scanning optical microscopes (NSOMs) are becoming increasingly popular analytical tools[8]. An NSOM instrument allow samples that are smaller than half the wavelength of light to be imaged by using an aperture size and an aperture-sample separation distance that is less than a wavelength of the source. Furthermore, because optical sources are utilized, NSOM

instruments provide this resolution while maintaining the advantages of traditional optical microscopes including nondestructive sample analysis, as well as spectroscopic analysis. The combination of NSOM with the synchrotron and MFC should speed near-field hyperspectral imaging and research into the etiology of AAA.

Collagen and elastin are major structural components of vessel walls that have been widely implicated in aneurysm formation, progression, and rupture[9]. The most prevalent structural modification associated with human AAAs that has been reported is a reduction in elastin concentration in the aortic wall. Significant correlations between reduced elastin concentration and AAA diameter have been observed. Alternatively, other studies have shown that reduction in elastin concentration is essentially complete prior to dilation of AAAs. One proposed mechanism for reduced elastin concentrations is degradation or loss brought about by elastolysis. Other work has reported that elastin content in the vessel walls of AAAs actually increases. In these studies, a 2.5-fold increase in elastin content was found in AAAs versus normal aortic samples of equal length. This increase, however, was accompanied by a significantly greater increase in total matrix proteins, which suggests that reduction in elastin content is at least in part due to dilution. These results and work by others suggest that an important mechanism in AAA formation is the regulation of matrix macromolecule synthesis.

Increased collagen concentration is another matrix modification that has been widely observed in human AAAs. Modifications in collagen organization and deposition have been correlated to rupture in human AAAs. Although there are noticeable differences in the findings of these studies, it is evident that increases in the collagen-to-elastin ratio are a general observation in AAAs.

Diffuse reflection near-infrared (near-IR) spectroscopy has proven to be a useful technique for identifying chemical content of biological tissues. Biological applications of near-IR spectroscopy include monitoring systemic and cerebral oxygenation and identifying plasma constituents including glucose, total protein, triglycerides, cholesterol, urea, creatinine, and uric acid. Our group has reported on the use of near-IR spectroscopy to classify human aortic atherosclerotic plaques and to identify cholesterol, HDL, and LDL in arterial wall samples[9,11].

Feasibility testing of NIR-NSOM with MFC to monitor collagen and elastin in the aortas of ApoE knockout mice with atherosclerosis and aneurysm formed from chronic infusion of the peptide angiotensin II has just begun. The goal of this project is to create a novel near-field microscopic probe capable of rapidly collecting molecular structural information from mouse aortas at subwavelength resolution. These data may help unravel the complex biochemistry of aneurysm formation and progression, and will certainly develop a new tool for use in other biomedical research.

Spatial Feature Encoding of Motion and Metabolism with Lenslet Arrays and Masks

In acute dosing experiments designed to test obesity theories, rats are given drugs and their activity, body temperature and oxygen consumption are monitored. Obligatory (basal metabolic) and facultative (work-related) thermogenesis can be established using these measurements. Our laboratory formerly employed an ordinary infrared/near-infrared InSb focal plane array video camera to monitor thermogenesis and metabolism in such rats (see Fig. 8).

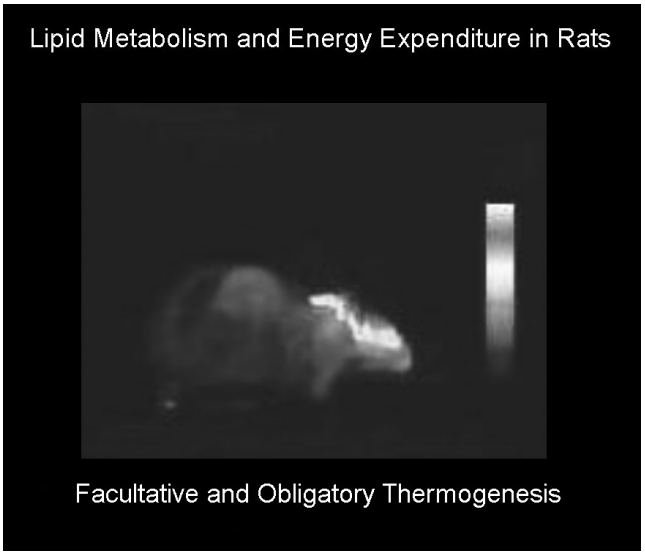

Fig. 8. Thermal infrared image of a freely moving rat obtained using an InSb focal plane array camera.

A half-dozen students with video recorders and computer workstations were needed with the traditional InSb camera system and imaging software to go through the video frame-by-frame to measure the movement of the rats (tracing and integrating the motion of their center of mass) and heat emission over time (thermogenesis). In this way, calories used in performing work and calories used in basal metabolism could be measured independently. In spite of the number of personnel and the expensive equipment dedicated to the project, it took weeks to analyze the data collected from a single one-hour experiment. Lenslet array cameras with limited spatial resolution can measure motion and heat emission with greater accuracy (i.e., better correlation to oxygen consumption) than can be obtained by manually circling image areas from a traditional IR camera and measuring subject motion and heat emission. The apparent reason for the increased accuracy is that there is more variation in how different students interpret rat motion and thermal emission than there is variation in the lenslet arrays. Furthermore, there is more variation in how the same student makes such measurements over days and weeks, than in how an ICI array encodes rat motion and thermal emission.

Differentiating between basal metabolism and work-related thermogenesis is important in studies of anti-obesity drugs because different drugs can increase metabolism in different ways. Some drugs increase metabolic rate and body temperature by agitating the subject and producing hyperactive behavior. Other drugs are pyrogenic and increase body temperature, but make the subject feel feverish and sick. The two types of reaction lead to very different movement behaviors.

Fig. 9 shows how lenslet array cameras can capture accurate temperature and motion data from a freely moving rat in a cage. A simple ICI camera with three apertures and only one IR detector behind the aperture mask easily permits rat motion and thermal emission to be measured by positioning four cameras around the cage: two on the x-axis (1.0 and 1.1, with lines of sight shown with solid lines), and two on the y-axis (0.0 and 0.1, dotted lines of sight). Each camera detector has three lines of sight that together cover a triangular zone in the cage. Two additional ICI cameras on the z-axis (2.0 and 2.1, with cylindrical lenses yielding planar fields of view represented by solid and dotted lines) monitor the height of standing and climbing movements.

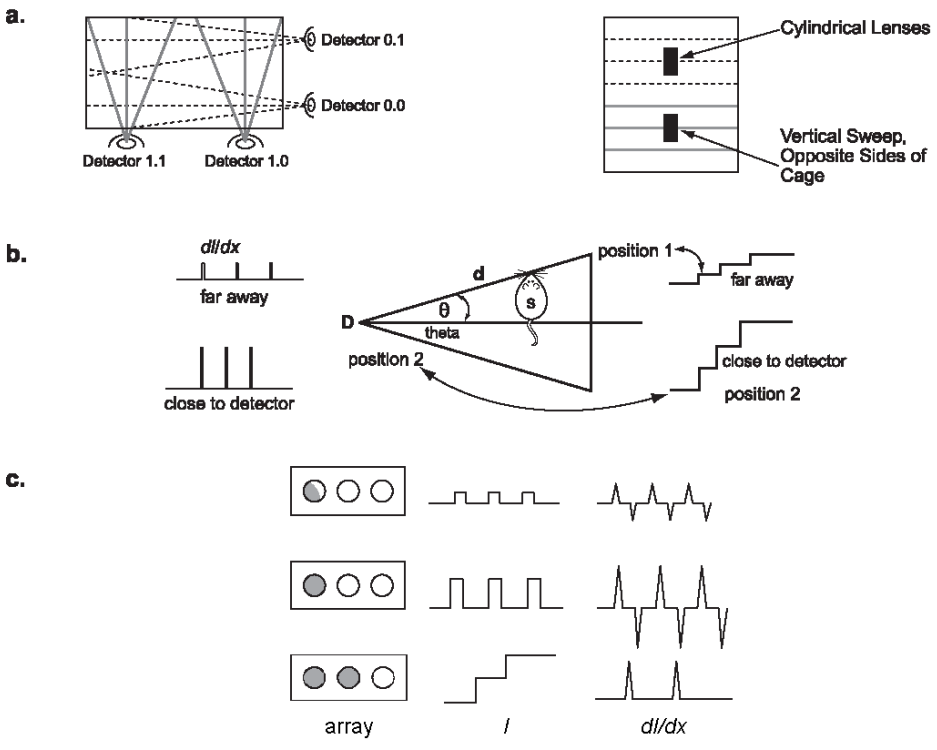

Fig. 9. ICI converts physical data fields into high-level information. a. layout of six ICI cameras around cage. b. rat distance from camera affects signal amplitude and timing. c. some lenslet codes for different rat locations and motions.

When a rat crosses in front of one of these cameras (see Fig. 9b), it can cross the field of view either close to the camera, or farther away. When the rat crosses close to the camera, it can illuminate all three apertures simultaneously. If the rat is very close to the camera, the signal increases in a stepwise fashion in relatively large steps. If the rat is not as close to the camera, the signal (with intensity *I*) increases in a stepwise fashion in relatively small steps.

When the rat crosses the field of view from very far away, it illuminates only one aperture in the mask at a time (see Fig. 9c, top row). Baseline detector drift can be a problem with thermal detectors. One way to eliminate excess drift is to modulate the signal, which in this case requires either active excitation or chopping the light at the aperture mask. Another way to correct detector baseline signal-drift is to use a detector amplifier operated in a high-pass filter configuration. In this configuration, the detector amplifier is differentiating, and the signal passed from the camera to the computer is the derivative of the stepwise signal (*dI/dx*). A simple low-speed A/D is all that is needed to interpret the camera data and calculate energy expenditure through basal metabolism and through work (work is done by the rat as it moves it body around in the cage). Using the derivative of the signal, there is no confusion between a rat crossing the field of view close to the camera or far away because, when the rat crosses close to the camera, there are no negative signal excursions until the rat begins to walk away. In contrast, when a rat crosses the field of view from far away, every positive signal excursion is followed immediately by a negative one.

Fig. 10 shows data collected from one ICI camera (thermal and motion measurement, in *dI/dx* format) measured over a one-hour period below the oxygen consumption data collected from the same cage. (The long measurement period causes the IR ICI pulse sequences to overlap.) The cage was a special metabolic container that was sealed except for one air inlet and one air outlet, and the incoming and outgoing air was monitored continuously. The graphs of data from the IR and O_2 sensors on the left of Fig. 10 reveal a clear correlation between thermal emission and oxygen consumption measurements. Where the IR measurement has the most ICI pulses, and where the IR measurement has the highest pulse heights, the oxygen consumption in the cage is also highest (i.e., total O_2 level is lowest at a constant airflow rate). Oxygen consumption is considered the "gold standard" for such metabolic measurements, but it cannot differentiate between oxygen consumption for basal metabolism and oxygen consumption for work-related thermogenesis. Instead, oxygen consumption serves as a measure of combined facultative and obligatory thermogenesis.

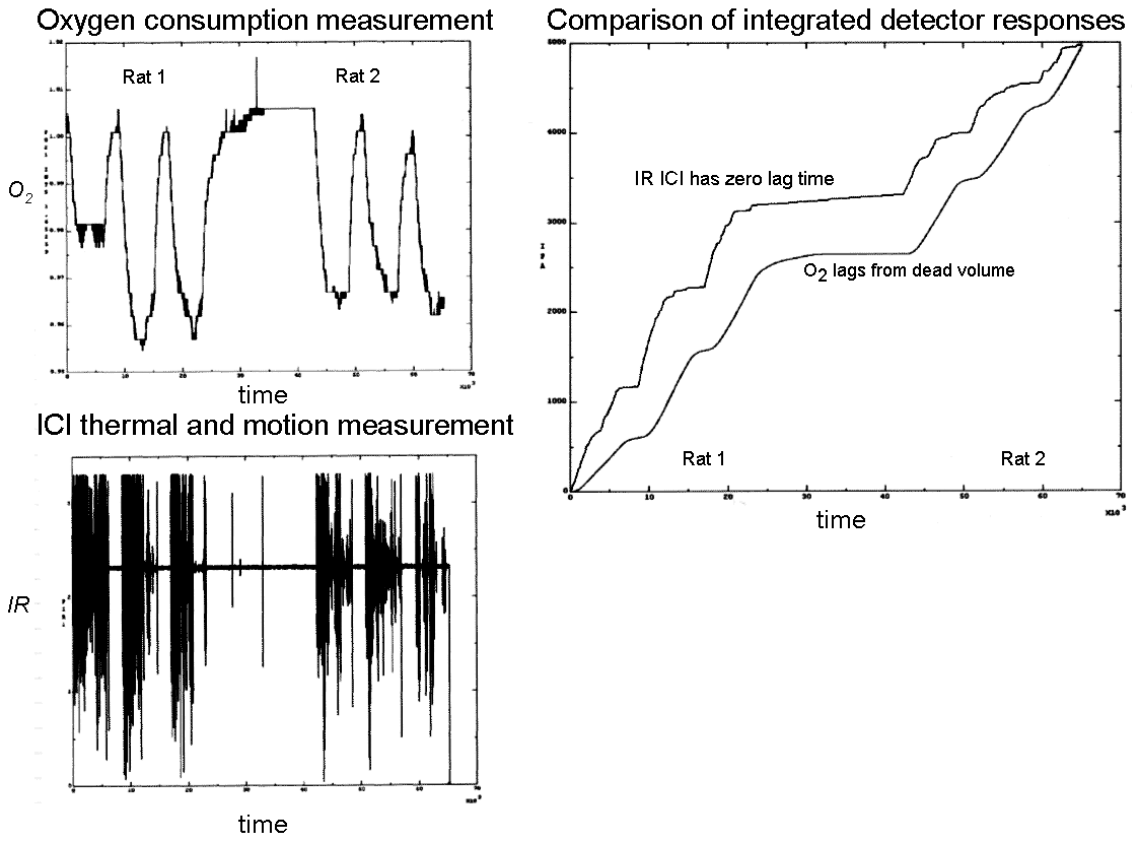

Fig. 10. Actual data from an ICI camera compares favorably to oxygen consumption data from the same cage.

The comparison of integrated detector responses on the right side of Fig. 10 reveals how well IR ICI tracks total metabolism more clearly. The upper curve was produced by ICI camera data, while the lower curve was calculated from O_2 sensor data. The correlation (r^2) between the two data series was 0.98. The correlation would be even higher were it not for the dead volume of the cage. The large cage volume creates a lag between subject activity and oxygen response, and reduces sensitivity to minor activity changes in the subjects.

Conclusion

The approaching tsunami in hyperspectral imaging is the speeding of processing and reduction of data storage requirements by downloading some of the computation to the detector array itself. In many cases, the detector array can perform both feature extraction (of both physical and spectral features) and encoding of these features. The codes are transmitted by the array to the computer, integrating the computation and imaging to reduce the huge data load and speed the processing. Molecular computing in a multiplex bandpass spectrometer can accomplish hyperspectral imaging as integrated computational imaging performs feature extraction.

The possibilities of the ICI approach are nearly endless. A synchrotron provides a bright, thin collimated beam of near-infrared and infrared light in the form of 20 ns pulses. This broadband beam of light can be readily coupled to a chalcogenide or other suitable optical fiber and used for NIR-NSOM (near-field scanning optical microscopy). Complex absorption filters can be used as mathematical factors to create a factor-analytic near-IR calibration in such a high-throughput near-IR nanospectrometer. The wavenumber (i.e., factor or principal component) selectors can be placed in the far field over the detector, simplifying construction. This new type of nanospectrometer offers simplicity, cost advantages, and enhanced throughput. The high-throughput wavelength selector is useful for ensuring the signal-to-noise ratio typically needed for chemometrics, and is vital given the extremely small aperture of a near-field probe. Using this device, collagen I and III as well as elastin can be imaged in aortas beyond the diffraction limit, enabling the mechanisms of collagen:elastin ratio increase in the genesis of aneurysms to be determined. Abdominal aortic aneurysms occur in 5-7% of people over age 60 in the United States[9]. Early intervention in the disease process could have a significant impact on the incidence of complications and on patient survival, but identifying incipient aneurysms can be difficult. ApoE knockout mice develop AAAs following infusion of angiotensin II by osmotic minipump into the subcutaneous space. These mice are used as models of AAA development, and their aortas will soon reveal much about the structure and composition of blood vessels that may clearly identify those at risk for life-threatening aneurysm.

ICI also has applications in coronary catheters, where physicians do not have much time to locate vulnerable atherosclerotic plaques. The “old western gunfight” analogy used earlier explains much of the motivation for ICI. A gunfighter who controls his revolver directly from his retina has some distinct advantages over a gunfighter who must send signals from his retina to his brain, and then from his brain to his gun hand. ICI has many military applications for the same reason – the available time to identify correctly many different targets is short. The data-analysis capabilities of computers continue to grow in accordance with Moore’s Law, and those capabilities need not be wasted on low-level operations. Moreover, significant developments in mathematical tools and innovations in optics manufacture permit more complex components to be made, such as molecular computing fiber optics and lenslet arrays. With the union of the latest computers and innovative optics, ICI is ready to reveal a universe of possibilities that have been concealed from the human eye.

Acknowledgements

This research was funded in part by KSEF-333-RDE-003, the NIH through HL58927, the NSF through DGE-9870691, and NIH and SESI through SC-NIAAA-93-01. The research is being carried out in part at the National Synchrotron Light Source, Brookhaven National Laboratory, which is supported by the U.S. Department of Energy, Division of Materials Sciences and Division of Chemical Sciences, under Contract No. DE-AC02-98CH10886.

References

1. Weiss, Peter. "New lenses create distorted images for digital enhancement." *Science News*, **163**(13), p. 200, 2003.
2. Thermogalactic, 2003. <http://www.galactic.com/>
3. DARPA, 2002. (http://www.darpa.mil)

4. DeVerse, R.A., Hammaker, R.M., Fateley, W.G. "Realization of the Hadamard Multiplex Advantage Using a Programmable Optical Mask in a Dispersive Flat-Field Near-Infrared Spectrometer." *Applied Spectroscopy.* **54**(12), 1751-1758, 2000.
5. CDM Optics, Inc. http://www.cdm-optics.com/
6. Buice, R.G., Jr., Lodder, R.A.. "Determination of Cholesterol Using a Novel Magnetohydrodynamic Acoustic-Resonance Near-IR Spectrometer." *Appl. Spectrosc.* **47**: 887-890, 1993
7. Fong, A. and Hieftje, G. M. "Near-IR Multiplex Bandpass Spectrometer Using Liquid Molecular Filters," *Applied Spectroscopy*, **49**(4), 493-498, 1995.
8. Symons, William Charles, Whites, Keith W., Lodder, Robert A.. "Theoretical and Experimental Characterization of a Near-Field Scanning Microwave Microscope (NSMM)". *IEEE Transactions on Microwave Theory and Techniques.* **51**(1): 91-99, 2003
9. Urbas, Aaron, Manning, Michael W., Daugherty, Alan, Cassis, Lisa A., Lodder, Robert A. "Near-Infrared Spectrometry of Abdominal Aortic Aneurysm in the ApoE -/- Mouse." *Anal. Chem.* **75**(14): 3650-3655, 2003
10. BNL, 2004. Brookhaven National Laboratory, <http://www.bnl.gov>.
11. Cassis LA, Lodder RA. Near-IR imaging of atheromas in living arterial tissue. Analytical Chemistry. **65**(9): 1247-56, 1993